



Synthesis, characterization, DFT studies, antibacterial, cytotoxic and molecular docking studies of 3-chloro-1-[(6-nitro-1, 3-benzoxazol-2-yl) amino]-4-phenylazetididin-2-one derivatives

S H Shreedhara¹, N D Jayanna^{2*}, T Manjuraj³, T C M Yuvaraj¹, Sarvajith M S⁴

¹ Department of Chemistry, Sahyadri Science College (Autonomous), Shimoga, Karnataka, India

² Department of Chemistry, KLE's Shri Shivayogi Murughendra Swamiji Arts, Science and Commerce College, Athani, Belagaum, Karnataka, India

³ Department of Chemistry, BEA's, DRM Science College, Davanagere, Karnataka India

⁴ Department of Chemistry, NMAM Institute of Technology, (Visvesvaraya Technological University, Belagavi) NITTE, Karnataka, India

Abstract

3-chloro-1-[(6-nitro-1, 3-benzoxazol-2-yl) amino] is a novel heterocyclic compound. IR, ¹H-NMR, ¹³C-NMR spectroscopic methods, and chemical analysis were used to discover -4-phenylazetididin-2-one derivatives. The 6-311++G (dp) basis set was used to optimise the molecular geometry of the synthesised compounds utilising the Density Functional Theory (DFT/B3LYP) approach in the ground state. The electrical and charge transport characteristics of synthesised compounds were used to determine the highest occupied Molecular Orbitals (HOMOs) and lowest unoccupied Molecular Orbitals (LUMOs). Frontier molecular orbitals, in addition to molecular electrostatic potential (MEP) (FMOs). On peripheral blood mononuclear cells (PBMCs), the cytotoxic activity of produced derivatives was examined, and the results were promising. The antioxidant activity of DPPH was investigated *in vitro*, with promising results. Furthermore, antibacterial assays with gram me positive and gram me negative bacteria strains, in combination with in silico docking interactions, suggest that the inhibitor has a high binding affinity for 2MGN, as evidenced by the ligand-receptor interaction.

Keywords: benzoxazole, schiff base, DFT. cytotoxicity, molecular docking

Introduction

Diseases caused by fungi and bacteria are the still major problems to the public health in spite of rapid progress in medicinal chemistry. Especially in following bacteria, drug resistance like methicillin-resistant *Staphylococcus aureus* (MRSA) and vancomycin resistant *Enterococci* (VRE) is of major concern. Benzoxazole derivatives have shown various biological activities such as antibacterial, antifungal [1-3], antimycobacterial [4], antitumor [5], HIV-1 reverse transcriptase [6] and topoisomerase I inhibitory activities. A benzoxazole derivative, calcimycin, is an ionophorus carboxylic polyether antibiotic obtained from *Streptomyces chartreusis* (NRRL 3882). It was found with the contrast of Gram-positive bacteria including some *Micrococcus* and *Bacillus* strains [7]. Rutiennocin, which is a spiroketalionophore antibiotic and isolated from a strain of *Streptomyces chartreusis* possessing a benzoxazole ring is initiated molecular structure found in Gram-positive bacteria. 2-Azetidinones, commonly known as β -lactams, are well-known heterocyclic compounds among the organic and medicinal chemists. The activity of the famous antibiotics such as penicillins, cephalosporins and carbapenems are attributed to the presence of 2-azetidione ring in them. Recently, some other types of biological activity besides the antibacterial activity have been reported in compounds containing 2-azetidione ring such biological activities include antimicrobial, anti-tubercular, carbonic anhydrase inhibitors, local anaesthetics, anti-inflammatory, anthelmintic, anticonvulsant, hypoglycemic

agents activity in the view of these observations, here we are presenting some target molecules of benzoxazole associated with Azitidine nucleus.

Materials and Methods

The chemicals and solvents were purchased from Sigma-Aldrich Co. (Durga chemicals, Mangalore, India). Silica gel HF254 chromatoplates (0.3 mm) were used for TLC and the mobile phase was chloroform/methanol (10:0.5) for compound 1. Melting point was recorded on a digital melting point apparatus instrument. The FT-IR spectrum was recorded using KBr pellets on a DR/Jasco FT-IR 6300 spectrometer. NMR spectra were recorded on a Varian Mercury 400 MHz NMR spectrometer (Manipal University, India) in CDCl₃ and dimethylsulfoxide (DMSO-d₆).

Tetramethylsilane (TMS) was used as an internal standard. The mass spectra were recorded on a Waters ZQ Micromass LC-MS spectrometer (Manipal University, India). Materials used in the microbiology study were: Mueller-Hinton Agar (Merck), Mueller Hinton Broth (Merck), Sabouraud Dextrose Agar (Merck), 96-well microplates, Transfer pipette, ampicillin, DMSO (Durga chemicals, Mangalore, India). Standard strains were: *Staphylococcus aureus* (ATTC-6538), *Bacillus cereus* (ATTC-11778), *Bacillus subtilis* (ATTC-6633), *Staphylococcus epidermidis* (ATTC-12228), *Pseudomonas aeruginosa* (ATTC-9027), *Salmonella typhimurium* (ATTC-23564) and *Escherichia*

coli (ATTC-8739) were purchased from Department of microbiology, NCL, Pune.

Synthesis of 2-hydrazinyl-6-nitro-1, 3-benzoxazole (4)

Compound 3 (3 gm) was taken in a round bottomed flask and treated with hydrazine hydrate (2. 2 ml) in ethanol (30 ml) and refluxed for 3 hours. ⁸ The reaction mixture was cooled and filtered. The obtained solid was recrystallized from ethanol to obtain the compound

Yield: 1. 8528 (62 %), m. p. 145-148⁰ C: IR (KBr, cm⁻¹): 3366 cm⁻¹ (NH₂) 3170 cm⁻¹ (NH): the ¹H-NMR (DMSO-d₆, δ ppm): 9. 05 (s, 1H, NH) 4. 6 (s, NH₂) (D₂O exchangeable), 7. 00-7. 4 (m, 3H, Ar-H): ¹³C NMR (DMSO-d₆, 100 MHz) δ. 115. 01-147. 07 (6C Ar-C): elemental analysis: calculated (%) for C₇H₆N₄O₃: C,45. 79; H,3. 29; N,22. 89: observed C,45. 72; H,3. 25; N,22. 86: M⁺194.

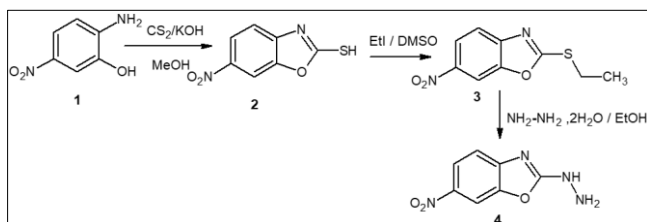


Fig 1: Synthetic route for the preparation of compound 42-[(2E) -2-benzylidenehydrazinyl]-6-nitro-1, 3-benzoxazole 6 (a)

To the solution of compound 4 (2 gm) in hot ethanol (30ml), substituted aldehydes 5 (a) (2.3 gm) and 3-4 drops of glacial acetic acid were added. The reaction mixture was refluxed for about 6 hr and cooled. The solid separated was filtered, washed with water, dried and recrystallized from ethanol to get 6 (a). The compounds 6 (b-f) can be prepared by following same procedure by using 5 (b-f) aldehydes.

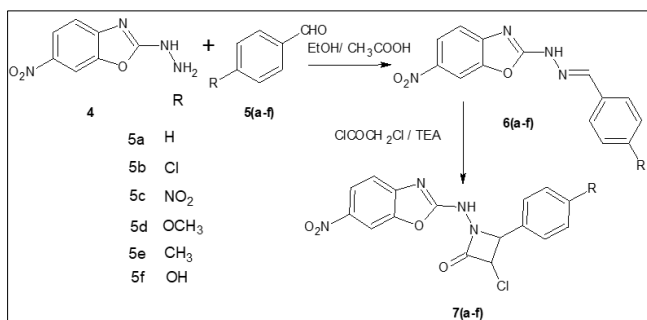


Fig 2: Synthetic route for the preparation of compound 7 (a-f) 3-chloro-1-[(6-nitro-1, 3-benzoxazol-2-yl) amino]-4-phenylazetidin-2-one 7 (a)

The compound 6 (a) (0.5 gm) was dissolved in 1, 4 Dioxane (20ml), treated with chloro acetyl chloride (0.35 gm) with few drops of tri ethyl amine (TEA) and refluxed for about 8 hr. then the reaction mixture was poured onto crushed ice. Solid product thus obtained was filtered, dried and recrystallized from ethanol to get compound 7 (a). The compounds 7 (b-f) can be prepared by following same procedure.

3-chloro-1-[(6-nitro-1, 3-benzoxazol-2-yl) amino]-4-phenylazetidin-2-one 7 (a)

Yield: 0. 3287 (75 %), m. p. 256-258⁰ C: IR (KBr, cm⁻¹): 1691 cm⁻¹ (C=O), 3423 cm⁻¹ (NH): the ¹H-NMR (DMSO-d₆, δ ppm):

9. 4 (s, 1H NH), 5. 38 (s, 1H, CH), 6. 83-7. 5 (m, 7H, Ar-H): ¹³C NMR (DMSO-d₆, 100 MHz) δ. 175 (C=O), 54 (CH), 119-151 (14C Ar-C): elemental analysis: calculated (%) for C₁₆H₁₁ClN₄O₄: C,53. 57; H,3. 09; N,15. 62: observed C,54. 72; H,3. 04; N,15. 50: M⁺,359, M⁺,361.

3-chloro-4- (4-chlorophenyl) -1-[(6-nitro-1, 3-benzoxazol-2-yl) amino]azetidin-2-one 7 (b)

Yield: 0. 3015 (68 %), m. p. 278-280⁰ C: IR (KBr, cm⁻¹): 1695 cm⁻¹ (C=O), 3436 cm⁻¹ (NH): the ¹H-NMR (DMSO-d₆, δ ppm): 9. 02 (s, 1H NH), 5. 2 (s, 1H, CH), 7. 24-8. 06 (m, 7H, Ar-H): ¹³C NMR (DMSO-d₆, 100 MHz) δ. 177 (C=O), 55 (CH), 118-158 (14C Ar-C): elemental analysis: calculated (%) for C₁₆H₁₀Cl₂N₄O₄: C,48. 88; H,2. 56; N,14. 25: observed C,48. 85; H,2. 50; N,14. 22: M⁺,393, M⁺,395, M⁺,397.

3-chloro-1-[(6-nitro-1, 3-benzoxazol-2-yl) amino]-4-(4-nitrophenyl) azetidin-2-one 7 (c)

Yield: 0. 3589 (76%), m. p. 265-267⁰ C: IR (KBr, cm⁻¹): 1693 cm⁻¹ (C=O), 3421 cm⁻¹ (NH): the ¹H-NMR (DMSO-d₆, δ ppm): 9. 2 (s, 1H NH), 5. 9 (s, 1H, CH), 7. 53-8. 54 (m, 7H, Ar-H): ¹³C NMR (DMSO-d₆, 100 MHz) δ. 171 (C=O), 59 (CH), 121-150 (14C Ar-C): elemental analysis: calculated (%) for C₁₆H₁₀Cl₂N₄O₄: C,47. 60; H,2. 50; N,17. 35: observed C,47. 57; H,2. 48; N,17. 32: M⁺,403, M⁺,405.

3-chloro-4- (4-methoxyphenyl) -1-[(6-nitro-1, 3-benzoxazol-2-yl) amino] azetidin-2-one 7 (d)

Yield: 0. 4240 (85%), m. p. 254-256⁰ C: IR (KBr, cm⁻¹): 1691 cm⁻¹ (C=O), 3423 cm⁻¹ (NH): the ¹H-NMR (DMSO-d₆, δ ppm): 9. 7 (s, 1H NH), 5. 8 (s, 1H, CH), 3. 7 (s, 3H, O-CH₃), 7. 25-8. 14 (m, 7H, Ar-H): ¹³C NMR (DMSO-d₆, 100 MHz) δ. 175 (C=O), 56 (CH), 42 (OCH₃) 122-152 (14C Ar-C): elemental analysis: calculated (%) for C₁₇H₁₃ClN₄O₅: C,52. 52; H,3. 37; N,14. 41: observed C,52. 49; H,3. 35; N,14. 36: M⁺,389, M⁺,391.

3-chloro-4- (4-methylphenyl) -1-[(6-nitro-1, 3-benzoxazol-2-yl) amino] azetidin-2-one 7 (e)

Yield: 0. 3846 (77%), m. p. 315-318⁰ C: IR (KBr, cm⁻¹): 1695 cm⁻¹ (C=O), 3434 cm⁻¹ (NH): the ¹H-NMR (DMSO-d₆, δ ppm): 9. 5 (s, 1H NH), 5. 8 (s, 1H, CH), 1. 5 (s, 1H, CH₃), 7. 05-8. 25 (m, 7H, Ar-H): ¹³C NMR (DMSO-d₆, 100 MHz) δ. 172 (C=O), 58 (CH), 28 (CH₃) 125-154 (14C Ar-C): elemental analysis: calculated (%) for C₁₇H₁₃ClN₄O₄: C,54. 78; H,3. 52; N,15. 03: observed C,54. 75; H,3. 48; N,14. 98: M⁺,373, M⁺,375.

3-chloro-4- (4-hydroxyphenyl) -1-[(6-nitro-1, 3-benzoxazol-2-yl) amino] azetidin-2-one 7 (f)

Yield: 0. 3305 (68%), m. p. 272-274⁰ C: IR (KBr, cm⁻¹): 1696 cm⁻¹ (C=O), 3454 cm⁻¹ (NH): the ¹H-NMR (DMSO-d₆, δ ppm): 9. 3 (s, 1H NH), 5. 8 (s, 1H, CH), 6. 8 (s, 1H, OH), 7. 18-8. 54 (m, 7H, Ar-H): ¹³C NMR (DMSO-d₆, 100 MHz) δ. 175 (C=O), 62 (CH), 122-158 (14C Ar-C): elemental analysis: calculated (%) for C₁₆H₁₁ClN₄O₅: C,51. 28; H,2. 96; N,14. 95: observed C,51. 25; H,2. 93; N,14. 91: M⁺,375, M⁺,377.

Microbiological Assay

The newly synthesized 3-chloro-1-[(6-nitro-1,3-benzoxazol-2-yl) amino]-4-phenylazetidin-2-one 7 (a-f) was tested for their antibacterial activity against *Staphylococcus aureus* (ATTC-

6538), *Bacillus cereus* (ATTC-11778), *Bacillus subtilis* (ATTC-6633), *Staphylococcus epidermidis* (ATTC-12228), *Pseudomonas aeruginosa* (ATTC-9027), *Salmonella typhimurium* (ATTC-23564) and *Escherichia coli* (ATTC-8739) bacterial strains was using agar well diffusion method.⁹ The 24 hr old Mueller-Hinton broth cultures of test bacteria were swabbed on sterile Mueller-Hinton agar plates using sterile cotton swab followed by punching wells of 6mm with the help of sterile cork borer. The standard drug (Amoxicillin, 30mg), compounds 7 (a-f) (20mg/mL of 10% DMSO) and control (10% DMSO) were added to the respectively labeled wells. The plates were allowed to stand for 30 minutes and were incubated at 37°C for 24 hr in upright position,

DPPH Scavenging Assay

The radical scavenging ability of synthesized compounds and the ascorbic acid (standard) was tested on the basis of radical scavenging effect on a DPPH free radical. Different concentrations (25, 50, 100, 200, and 400 µg/mL) of compounds and standard were prepared in methanol. In clean and labeled test tubes, 3 mL of DPPH solution (0.002% in methanol) was mixed with 25, 50, 100, 200, and 400 µg/mL concentrations of compounds and standard separately and make up the solution up to 4 mL by adding methanol. The tubes were incubated at room temperature in dark for 30 minutes and the optical density was measured at 517 nm using UV-Visible Spectrophotometer. The absorbance of the DPPH control was also noted. The scavenging activity was calculated using the formula. Scavenging activity (%) = $A - B/A \times 100$, where *A* is the absorbance of DPPH and *B* is the absorbance of DPPH in standard combination^[10].

Cytotoxic activity

Preparation of peripheral blood mononuclear cells (PBMCs) or buffy coat

Blood samples from healthy volunteers were collected by venipuncture and transferred into 2 ml heparin coated vacutainers. It was diluted to 1:1 ratio with PBS (Phosphate buffer solution, pH 7.0) layered onto 4 mL Ficoll without getting mixed up. It was further separated by centrifuging at 1,000 rpm for 30 min at room temperature. During the centrifugation the PBMCs move from plasma and suspend as the density gradient. Plasma was removed down to 1 cm above buffy coat and discarded the white layer lying on top of the red cells. The buffy coat layer was washed twice with PBS. Roswell Park Memorial Institute (Gibco, Life Technologies) medium was prepared by mixing 10 mL of Fetal bovine serum (Invitrogen) and 200µL antimycotic [Antibiotic antimycotic solution with Streptomycin (10mg/20mL), 10,000 U Penicillin, Amphotericin B and 0.9% normal saline]. This mixture (4mL) was dispensed into falcon tubes, 30µL of Phytohemagglutinin (Invitrogen) and 200µL of PBMCs were incubated at the atmosphere of 95% air and 5% CO₂ at 37°C for 4 hr^[11].

About 10 µg/mL, 50 µg/mL and 100 µg/mL of the selected compounds (1mg/mL) were added to the respectively labeled PBMCs tubes and incubated for 72 hr at the earlier mentioned conditions. After 72 hr, cell viability was determined by the trypan-blue dye exclusion method¹².

Trypan blue exclusion test cells were clarified by centrifuging at 1000 rpm for 30 min at room temperature. The supernatant liquid was discarded and to the solution 10µL of PBMCs, 10µL of

trypan blue was added and incubated for 10 min at room temperature. About 10µL of incubated sample was loaded on previously cleaned Haemocytometer and counted the number of live cells, total cells and dead cells at four corners under Trinocular microscope, Nikon Eclipse E200.

Computational studies

Calculations of the title compound were carried out with Gaussian 09 software¹³ using B3LYP/6-311++G (d, p) (5D, 7F) basis set to predict the molecular structure. This basis set was chosen particularly because of its advantage of doing faster calculations with relatively better accuracy and structures and it contains both soft and polarisation functions and it has proven to yield reliable descriptions of the molecular structure^[14,15]. As the DFT hybrid B3LYP functional tends to overestimate the wavenumbers of the fundamental modes, a scaling factor of 0.9613 has been uniformly applied to the calculated wavenumbers. The assignments of the calculated wavenumbers are aided by the animation option of GAUSSVIEW program and potential energy distribution by GAR2PED soft-ware package. The theoretically optimized geometrical parameters are given in table 4.

Result and Discussion

Chemistry

The compound 2-amino-5-nitrophenol **1** were treated with carbon disulphide and potassium hydroxide in the presence of ethanol as solvent to give a compound 6-nitro-1, 3-benzoxazole-2-thiol **2**. To the compound **2** were treated with iodoethane in the presence of sodium hydroxide, DMSO used as a solvent to get 2-(ethylsulfanyl) -6-nitro-1,3-benzoxazole **3**, then the compound **3** were reacted with hydrazine hydride by using ethanol solvent to get intermediate compound 2-hydrazinyl-6-nitro-1,3-benzoxazole **4** (Scheme 1). The compound **4** was characterized by ¹H NMR, which exhibited two singlet's at δ4.60, δ9.05 for –NH₂ and –NH protons, respectively (D₂O exchangeable). Which is used as a intermediate compound to synthesis of targeted molecule **7** (a-f).

The derivatives **6** (a-f) were synthesized using 2-hydrazinyl-6-nitro-1,3-benzoxazole **4** were treated with different aldehyde **5** (a-f) to forms a Schiff's base, which can be confirmed by IR spectrum 1614 cm⁻¹ for N=CH and ¹H NMR shows δ12.00 (s, N=CH) which confirms the disappearance of one proton in NH₂ of the compound **4**.

The Schiff's base derivatives **6** (a-f) were treated with Chloro acetyl chloride in the presence of 1, 4 dioxane with few drops of TEA to forms a different derivatives of azetidines target molecules **7** (a-f). Which can be confirmed by IR, ¹H NMR, mass, and elemental analysis. IR spectrum shows 1691 cm⁻¹ for (C=O), 3421cm⁻¹ for (NH) and ¹H NMR shows δ 6.95-7.80 (m, 7H, Ar-H), 9.4 (s, 1H NH), 5.3 (s, 1H CH). Which confirms the disappearance for N=CH and forms cyclized azetidines ring. The Mass spectra's are concurrence with Molecular weights of the target compounds (Figure 2).

Geometrical parameters

The optimized molecular structure of the title compound **3d** (Fig 3) was determined by using Gaussian 09 program and the optimized geometry. From the table 1 the C-C bond length is C1-C2 (1.386 Å) lesser than that of C13-C14 (1.540 Å) because of the delocalization of electron density of C1-C2 with the phenyl

ring. Also C20-C123 (1.770 Å), C6-N10 (1.470 Å), N11-N12 (1.450 Å), C19-O24 (1.440 Å) and C21-O22 (1.220 Å) bond lengths are different because of the difference in their environment (figure 4). The bond angle C1-N7-C8 (104.00) and

N7-C8-O9 (108.57) indicates the π bond character of the former. Also C20-C21-O22 (105.07) and N12-C21-C20 (93.72) indicates slightly higher electronegative property of oxygen and nitrogen atom with π bond [16].

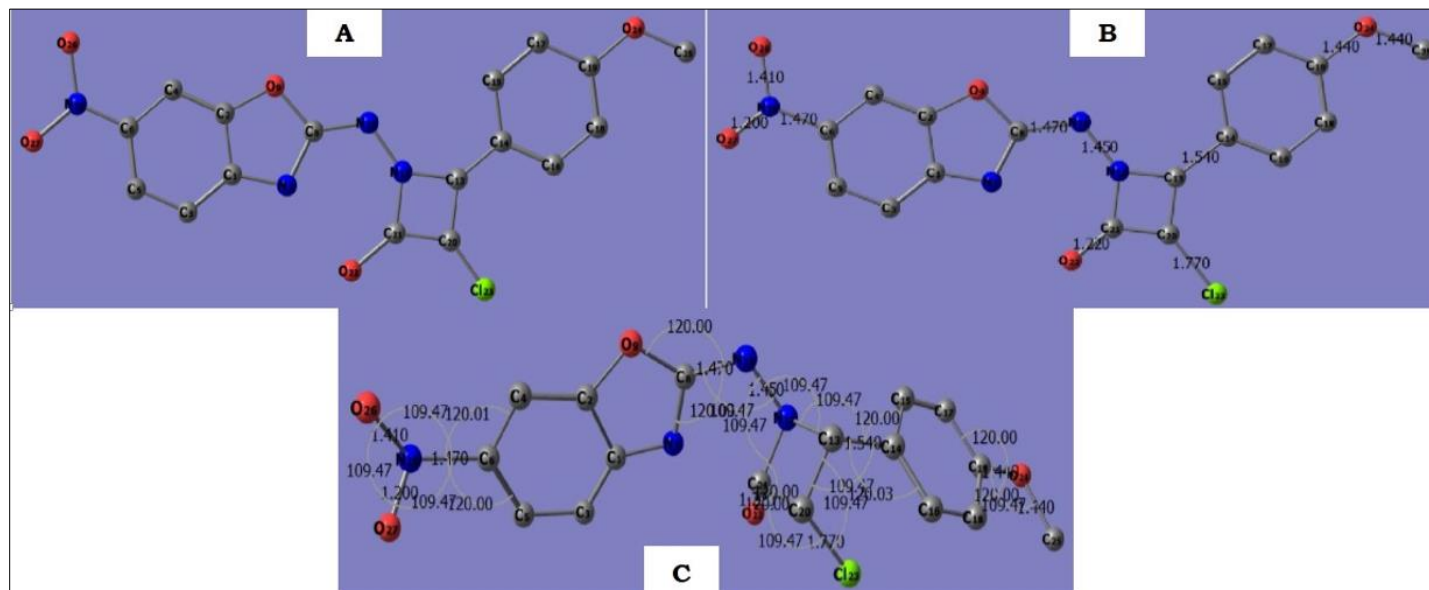


Fig 3: (A) Optimised geometry of the compound 3d, (B) Selected bond length (Å) of compound 3d, (C) Selected bond angle (degree) of compound 3d

Table 1: Selected bond length (Å) and bond angle (degree) of compound 3d

Bond length	(Å)	Bond Angle	(°)
C (1) -C (2)	1.386	C (1) -N (7) -C (8)	104.000
C (1) -C (3)	1.386	N (7) -C (8) -O (9)	108.573
C (1) -N (7)	1.446	N (7) -C (8) -N (11)	125.712
C (2) -C (4)	1.386	O (9) -C (8) -N (11)	125.712
C (2) -O (9)	1.410	C (2) -O (9) -C (8)	86.294
C (6) -N (10)	1.446	C (6) -N (10) -O (26)	119.999
N (7) -C (8)	1.244	C (6) -N (10) -O (27)	120.000
C (8) -O (9)	1.841	O (26) -N (10) -O (27)	119.999
C (8) -N (11)	1.446	N (11) -N (12) -C (21)	134.999
N (10) -O (26)	1.316	N (12) -C (13) -H (37)	109.500
N (10) -O (27)	1.132	C (14) -C (15) -C (17)	120.000
N (11) -N (12)	1.352	C (14) -C (15) -H (34)	119.999
N (11) -H (38)	1.028	C (17) -C (15) -H (34)	119.999
N (12) -C (13)	1.446	C (14) -C (16) -C (18)	120.000
N (12) -C (21)	1.446	C (16) -C (18) -H (31)	119.998

Frontier molecular orbital analysis

It is important that ionization potential (I), electron affinity (A), electro philicity index (ω), chemical potential (μ), electronegativity (χ) and hardness (η) to be put into a molecular orbital frame work. Based on density functional descriptors, global chemical reactivity descriptors of compounds such as hardness, chemical potential, softness, electro negativity and electrophilicity index as well as local reactivity has been defined [17, 18]. Using Koopman's theorem for closed shell components η , μ and χ can be defined as $\eta = (I - A) / 2$; $\mu = - (I + A) / 2$; $\chi = (I + A) / 2$; where I and A are the ionization potential and electron affinity, respectively. The ionization energy (I) and electron affinity (A) can be expressed through HOMO and LUMO orbital energies as $I = E_{\text{HOMO}} = -7.0889$ eV and $A = E_{\text{LUMO}} = -3.0703$ eV for the compound 3d. Electron affinity refers to the capability of ligand to accept precisely one electron from a donor. However, in many kinds of bonding *viz.* covalent hydrogen bonding, partial charge transfer takes place. Considering the chemical hardness (η), large HOMO-LUMO energy gap (ΔE) means a hard molecule and small HOMO-LUMO gap means a soft molecule. One can also relate the stability of the molecule to hardness, which means that the molecule with smaller HOMO-LUMO gap is more reactive. For the title compound, the energy gap is 4.0186 eV respectively. Parr *et al* [19]. have defined a new descriptor to quantify the global electrophilic power of the compound as electrophilicity index (ω) which defines a quantitative classification of global electrophilic nature of a compound. Parr *et al.* have proposed electrophilicity index (ω) as a measure of energy lowering due to maximal electron flow between donor and acceptor. They defined electrophilicity index as follows: $\omega = \mu^2 / 2\eta$. The usefulness of this new reactivity measure has been recently demonstrated in understanding the toxicity of various pollutants in terms of their reactivity and site selectivity²⁰. The calculated values, of ω , μ , χ and η are 6.422, 5.0796, -5.0796 and 2.009 eV for compound 3d. The calculated value of electrophilicity index describes the biological activity of the title compound. The atomic orbital components of the frontier molecular orbital are shown in Fig 4.

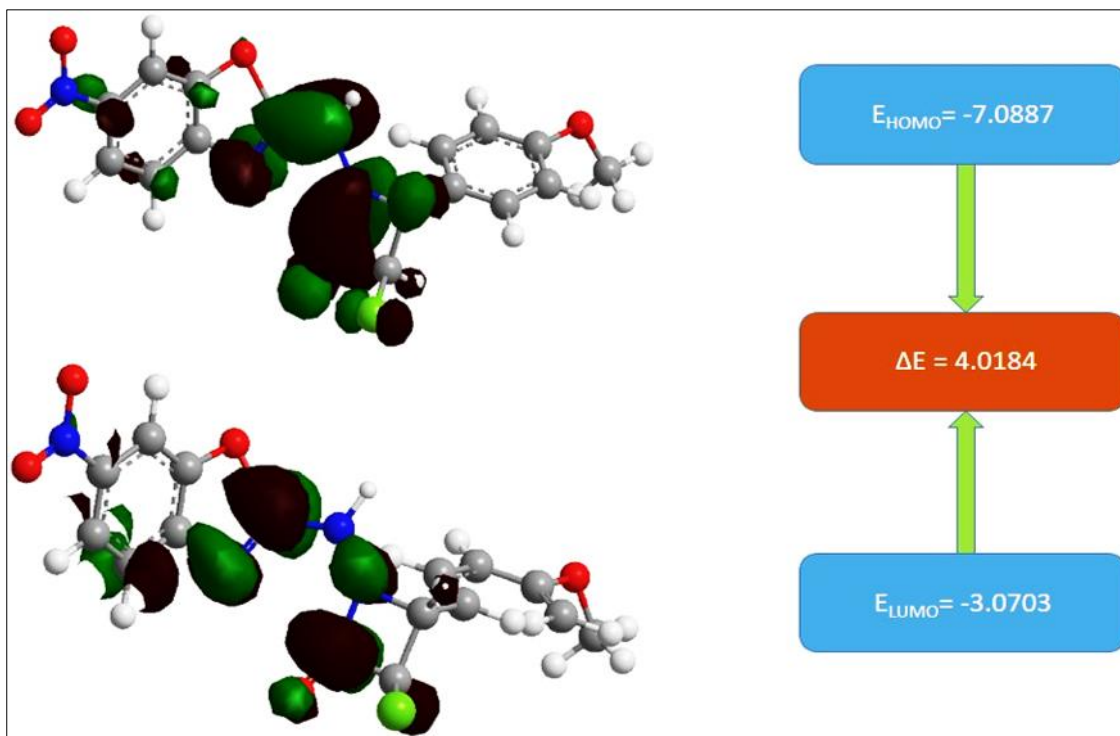


Fig 4: Molecular orbital diagram with HOMO and LUMO orbital of Compound 3d

The DFT/B3LYP method indicates the chemical reactivity and the selection of active sites of the molecular system. The energy of FMOs and the energy band gap explain the charge transfer interaction within the molecule. The chemical reactivity values as electronegativity (χ), chemical potential (μ), global hardness (η), global softness (S) and global electrophilicity index (ω)^[21, 22] are listed in Table 2.

$$\chi = (ELUMO + EHOMO) / 2$$

$$\mu = -\chi = (ELUMO + EHOMO) / 2$$

$$\eta = (ELUMO - EHOMO) / 2$$

$$S = 1/2\eta$$

$$\omega = \mu^2/2\eta$$

$$\sigma = 1/\eta$$

Table 2: Calculated quantum chemical parameters for compound 3d

Compound	Homo in eV	Lumo in eV	ΔE in eV	χ Pauling	η in eV	σ	μ in eV	S	ω eV
3d	-7.0889	-3.0703	4.0184	-5.0796	2.009	0.4977	-5.0796	0.2488	6.422

Molecular electrostatic potential (MEP)

MEP is related to the electron density and is a very useful descriptor in understanding sites for electrophilic and nucleophilic reactions^[23]. To predict reactive sites of electrophilic and nucleophilic attacks for the title compound, MEP at the B3LYP/6-311++G (d,p) (5D, 7F) optimized geometry was calculated.

The negative (red) regions of MEP were related to electrophilic reactivity and the positive (blue) regions to nucleophilic reactivity (Fig 5).

From MEP it is evident that the negative charge covers the O atoms of Cl group, N atom of benzoxazole group and the positive region is over the N group azetidin.

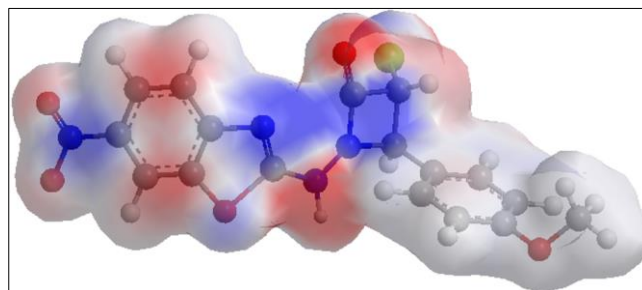


Fig 5: MEP plot of compound 3-chloro-4-(4-methoxyphenyl)-1-[(6-nitro-1,3-benzoxazol-2-yl)amino]azetidin-2-one 3d

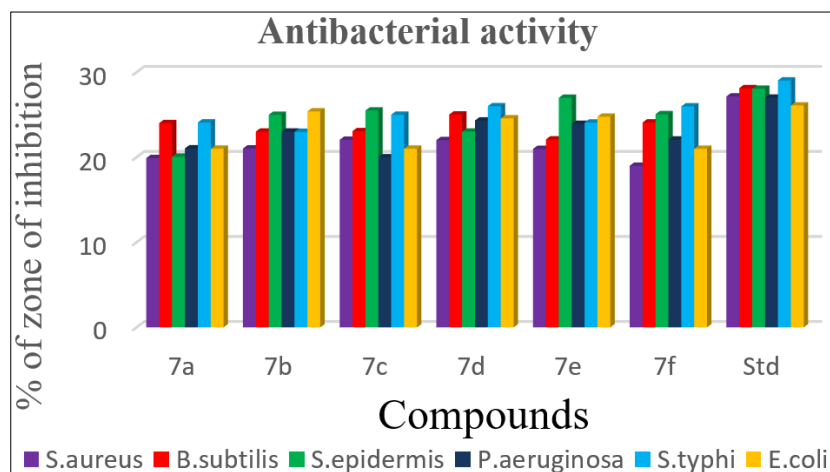
Antibacterial activities

The synthesized compounds were assayed *in vitro* for antibacterial activity against *Staphylococcus aureus* (ATCC-6538), *Bacillus cereus* (ATCC-11778), *Bacillus subtilis* (ATCC-6633), *Staphylococcus epidermidis* (ATCC-12228), *Pseudomonas aeruginosa* (ATCC-9027), *Salmonella typhimurium* (ATCC-23564) and *Escherichia coli* (ATCC-8739). For comparison of the antimicrobial activity, ampicillin were used as the reference antibacterial agents^[24].

In this study, our goal was to investigate the role of efficiency substitution on the two positions with a nitro substituted benzoxazole group linked with azitidine ring for antimicrobial activity. The compound 7c, 7d and 7f indicated a broad antibacterial activity against some *Staphylococcus epidermidis*, *Salmonella typhimurium*. The compound 7a, 7b and 7e was less active than the compared reference drugs against these Gram-negative bacteria and represents in Fig 6 and Table 3. The tested compound 7c, 7d and 7f possessed potent activity against *Staphylococcus epidermidis* and *Salmonella typhimurium* due to presence of NO₂, OCH₃ and OH substituents than compared to other derivatives.

Table 3: Antibacterial activity of compounds 7 (a-f)

Compounds	Zone of inhibition in mm					
	Gram positive bacteria			Gram negative bacteria		
	<i>S. aureus</i>	<i>B. subtilis</i>	<i>S. epidermis</i>	<i>P. aeruginosa</i>	<i>S. typhi</i>	<i>E. coli</i>
7a	19.90±0.32	24.01±0.65	20.07±0.25	21.04±0.31	24.09±0.63	21.00±1.01
7b	21.03±0.33	23.02±0.75	24.99±0.90	23.01±0.0	22.99±0.22	25.39±0.77
7c	22.05±0.88	23.07±0.64	25.50±0.42	20.00±0.98	25.00±0.98	21.00±0.98
7d	22.02±0.12	25.02±0.00	23.02±0.66	24.32±0.85	26.00±0.99	24.57±0.45
7e	20.98±0.29	22.09±0.75	26.99±0.24	23.92±0.37	24.08±0.22	24.77±0.26
7f	19.00±0.78	24.09±0.76	25.06±0.0	22.08±0.43	25.98±0.56	20.99±0.66
Std Amoxicillin	27.15±0.98	28.12±0.12	28.06±0.36	27.00±0.88	29.03±0.44	26.09±0.36

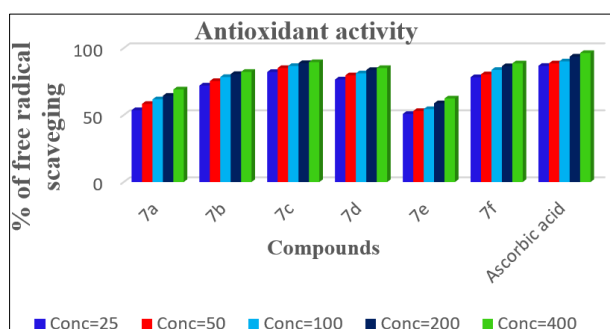
**Fig 6:** Antibacterial activity of compounds 7 (a-f)**Antioxidant activity**

The antioxidant activity at different concentrations, namely, 25, 50, 100, 200, and 400 $\mu\text{g/mL}$, of the compounds 7 (a-f) and ascorbic acid was tested on the basis of the radical scavenging effect of the stable DPPH free radical assay [25]. The compound

7c and 7f showed better radical scavenging activity followed by the compound 7d and 7b and are represented in the Fig 7 and Table 4.

Table 4: Antioxidant activity of synthesized compounds 7 (a-f)

Compounds	Scavenging activity of different concentration ($\mu\text{g/mL}$) in %				
	25	50	100	200	400
7a	53.67	58.30	61.71	64.38	69.09
7b	72.02	75.36	78.41	80.63	82.25
7c	82.16	85.10	86.63	88.78	89.48
7d	76.56	79.67	81.12	83.63	85.10
7e	50.81	53.00	54.40	58.78	62.38
7f	78.25	80.43	83.71	86.45	88.53
Ascorbic acid	86.71	88.57	90.04	93.62	96.33

**Fig 7:** Antioxidant activity of synthesized compounds 7 (a-f)**Cytotoxic activity**

Peripheral Blood Mononuclear Cells (PBMCs) was used as the cell line in this study. The synthesized compounds 7c, 7d and 7f were exhibited potent antibacterial activity, hence those compounds were selected and screened for their cytotoxic activity. Each compound was tested at three different concentrations 10 $\mu\text{g/mL}$, 50 $\mu\text{g/mL}$ and 100 $\mu\text{g/mL}$ against PBMCs cell line [26]. The compound 7d displayed highest 78.40 % of non-cell viability at 100 $\mu\text{g/mL}$ concentration, then compound 7f showed 72.05 % non-cell viability at 100 $\mu\text{g/mL}$ concentration followed by the compound 7c exhibited 75.26 % non-cell viability at 50 $\mu\text{g/mL}$ concentration.

Table 5: Cytotoxic activity of newly synthesized derivatives against PBMCs.

Sample	Total cells	Live cells	Dead cells	% of Cells viability	%of cells non-viability
7c-10 μ g/mL	78	29	49	37.1	62.8
7c -50 μ g/mL	82	38	44	46.3	53.7
7c -100 μ g/mL	186	46	140	24.73	75.26
7d-10 μ g/mL	82	32	50	39.02	60.97
7d -50 μ g/mL	212	60	142	28.3	66.98
7d -100 μ g/mL	125	27	98	21.60	78.40
7f-10 μ g/mL	90	42	48	46.66	53.33
7f-50 μ g/mL	136	38	98	27.94	72.05
7f-100 μ g/mL	92	68	24	73.91	26.08
Control	118	17	101	14.4	85.5

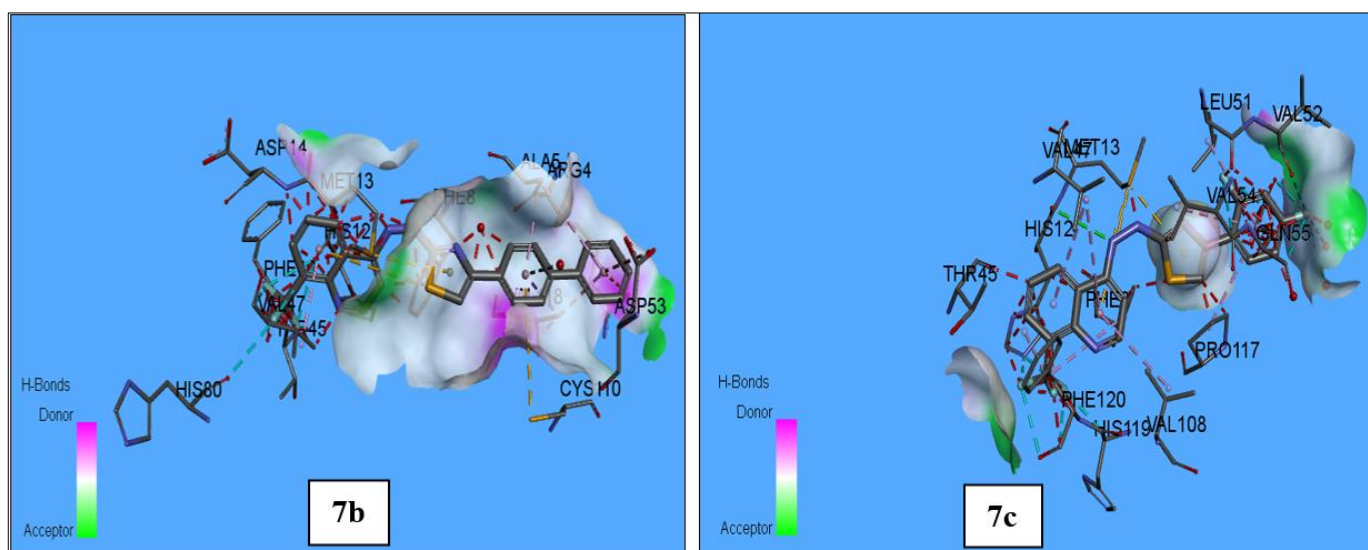
Molecular docking studies

Molecular docking is an efficient tool to get an insight into ligand-receptor interactions. All molecular docking calculations were performed on Auto-Dock-Vina software [27]. Water molecules and co-crystallized ligands were removed and the ligand was prepared for docking by minimizing its energy at B3LYP/6-311++G (d, p) (5D, 7F) level of theory. The active site of the enzyme was defined to include residues of the active site within the grid size of 40 Å 40 Å 40 Å. Lamarckian Genetic Algorithm (LGA) available in Auto Dock Vina was employed for docking. The docking protocol was tested by removing co-crystallized inhibitor from the protein and then docking it at the same site. To evaluate the quality of docking results, the common way is to calculate the Root Mean Square Deviation (RMSD) between the docked pose and the known crystal structure confirmation. RMSD values up to 2 Å are considered reliable for the docking protocol. The docking protocol we employed predicted a similar confirmation with RMSD value well within the allowed range of 2 Å (Fig. 8 and 9). Docking study of the synthesized compounds 7 (a-f) were evaluated against the receptor (Pdb: 3MGN). In the present study, an effort was made to evaluate their antioxidant behavior, we have selected receptor (Pdb: 3MGN) to obtained docking scores (binding interaction energy) [28]. The results were tabulated in Table 6 and interaction modes are shown in figure 8. The synthesized molecules 7 (a-f) binds with various amino acids in the receptor (Pdb: 3MGN) in

the active pocket sites and given a molecular interaction energy (E-total value) in range of -244.10 to -271.12 (Kcal/mol). The benzoxazole linked azetidine compounds such as 7b, 7c and 7d showed higher binding energy as compared with the compounds 7a, 7e and 7f. The confirmation which was close to the confirmation of co-crystallized ligand scored well was visualized for ligand-protein interactions in Discover Studio Visualizer 4.0 and pymol software. The ligand binds at the active sites of the protein by weak non-covalent interactions most prominent of which are H-bonding, alkyl-p and van der waals interactions. Amino acids *viz.* ASN: 278, MET: 277 and PRO: 67 form H-bonds with the ligand Figure 8 and 9. The residues PROA: 67 hold the benzoxazole rings of the compound by alkyl-p interactions. The ASPA: 275 is involved in a vanderwaals interaction with the ligand.

Table 6: Docking result of synthesized compounds in the binding site of receptor.

Entry	Receptor PDB code	ΔG (Kcal/mol)
7a	3MGN	-253.19
7b	3MGN	-266.41
7c	3MGN	-271.12
7d	3MGN	-266.41
7e	3MGN	-259.13
7f	3MGN	-244.10

**Fig 8:** 3D Interactions of compounds 7b and 7c with receptor (PDB: 3MGN).

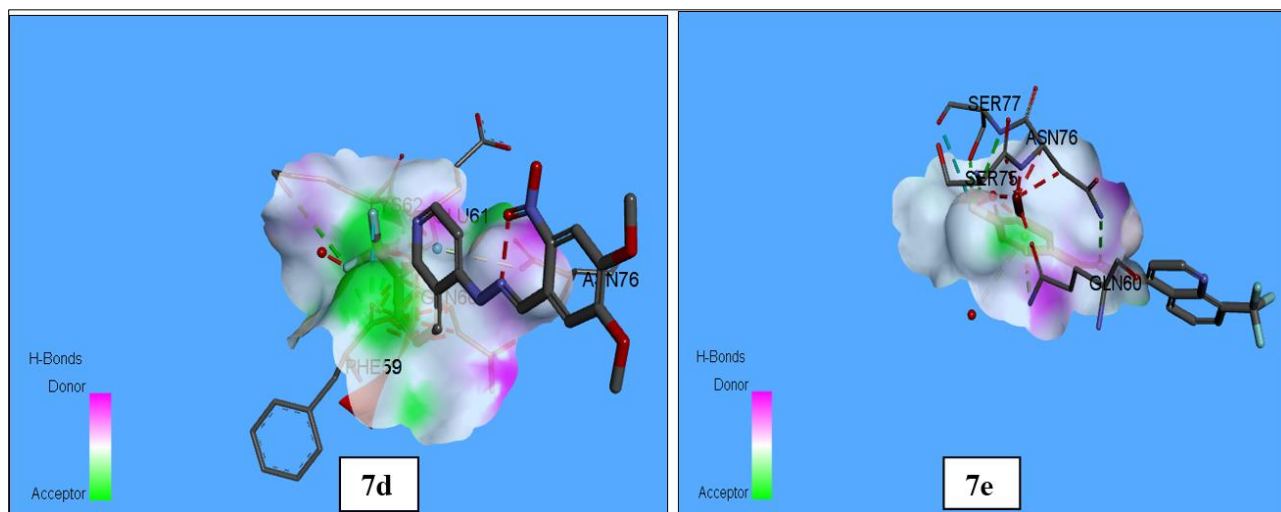


Fig 9: 3D Interactions of compounds 7d and 7e with receptor (PDB: 3MGN).

Conclusion

In this study, synthesis, antibacterial, antioxidant and cytotoxic activities of 3-chloro-1-[(6-nitro-1,3-benzoxazol-2-yl)amino]-4-phenylazetidin-2-one derivatives 7 (a-f) is reported. The molecular structural parameters have been obtained using density functional theory. The synthesized molecules were evaluated by IR, ^1H NMR, LCMS and ^{13}C NMR analytical techniques. The title compound possessed potent antibacterial activity against some *Staphylococcus epidermidis*, *Salmonella typhimurium*. The compound 7c and 7f showed higher free radical scavenging activity, the nitro, methoxy and hydroxyl substituted title compound exhibited potent non-cell viability against PBMCs cell lines and the binding free energy of the synthesized compounds were predicted by Auto dock Vina suggests good binding affinity at 244.10 to -271.12 Kcal/mol.

Acknowledgement

The authors are grateful to the Principal, Sahyadri Science College, Shivamogga, for laboratory facilities to carry out research work. The authors are also thankful to MIT, Manipal and IIT Bombay for providing ^1H NMR and ^{13}C NMR spectral facilities. We are also thankful to the Department of Microbiology and Cell Biology IISc Bangalore, India for their support in carrying out molecular docking study.

References

1. Elmegeed GA, Khalil WKB, Mohareb RM, Ahmed HH, Abd-Elhalim MM, Elsayed GH. Cytotoxicity and gene expression profiles of novel synthesized steroid derivatives as chemotherapeutic anti-breast cancer agents. *Bioorg Med Chem*,2011;19:6860-6872.
2. Hussain Z, Yousif E, Ahmed A, Altaie A. Synthesis, characterization of Schiff's bases of sulfamethoxazole, *Org Med Chem Lett*,2014;4:1-9
3. Lee HW *et al.* Molecular design, synthesis, and hypoglycemic and hypolipidemic activities of novel pyrimidine derivatives having thiazolidinedione. *European Journal of Medicinal Chemistry*,2005;40 (9):862-874.
4. Balkan A, Ertan M, Burgemeister T. Synthesis and Structural Evaluations of Thiazolo [3, 2 - a]pyrimidine Derivatives. *Archiv der Pharmazie*,1992;325 (8):499-503.
5. Pandey S, Pandey P, Singh J. Synthesis, characterization and fungicidal activity of N- (5-oxo-3,7-diaryl-6,7-dihydro-5H-thiazolo[3,2,a] pyrimidin-6-yl) benzamide derivatives. *Der Pharma Chemica*,2014;6 (1):170-175.
6. Hwang HS, Moon EY, Seong SK, Choi CH, Chung SH. Characterization of the anticancer activity of DW2282, a new anticancer agent. *Anticancer Res*,1999;19:5087-5093.
7. Lima PC, Lima LM, Silva KC, Leda PH *et al.* Synthesis and analgesic activity of novel N-acyl-aryl-hydrazones and isosters, derived from natural safrole. *Eur J Med Chem*,2000;35:187-203.
8. Madhavi R, Mohana Krishna A, Shobha Rani G, Mounika D. Isoniazid: A Review of Analytical Methods *Asian J Pharm Ana*,2015;5 (1):41-45.
9. Przybylski P, Huczynski A, Pyta K, Brzezinski B, Bartl F. Biological properties of schiff bases and azo derivatives of phenols, *Curr. Org. Chem*,2009;13:124-148.
10. Medina JC, Shan H, Beckmann RP, Farrell DL, Clark RM. Novel antineoplastic agents with efficacy against multidrug resistant tumor cells. *Bioorg Med Chem Lett*,1998;8:2653-2656.
11. Kinnula VL, Crapo JD. Superoxide dismutases in malignant cells and human tumors, *Free Radic. Biol. Med*,2004;36:718-744.
12. Jayanna ND, Vagdevi HM, Dharshan JC, Raghavendra R, Telkar SB. Synthesis, Antimicrobial, Analgesic Activity and Molecular docking studies of novel 1- (5,7-dichloro-1,3-benzoxazol-2-yl) -3-phenyl-1H-pyrazole-4-carbaldehyde derivatives, *Med Chem Res*,2013;22:5814-5822.
13. Ravi kumar C, Joe IH, Jayakumar VS. Charge transfer interactions and nonlinear optical properties of pushpull chromophore benzaldehyde phenylhydrazone: a vibrational approach, *Chem. Phys. Lett*,2008;460:552-558.
14. Chocholousova J, Spirko V, Hobza P. First local minimum of the formic acid dimer exhibits simultaneously red-shifted OH-O and improper blue-shifted CH-O hydrogen bonds, *Phys. Chem. Chem. Phys*,2004;6:37-41.
15. Dharmaraj N, Viswanathamurthi P, Nataraj K. Ruthenium (II) complexes containing bidentate Schiff bases and their antifungal activity, *Transit. Met. Chem*,2001;26:105-109.

16. Gulcin I, Dastan A. Synthesis of dimeric phenol derivatives and determination of *In vitro* antioxidant and radical scavenging activities, *J. Enzym. Inhib. Med. Chem.*,2007;22:685-695.
17. Manjuraj T, Krishnamurthy G, Yadav Bodke D, Bhojya Naik HS. Synthesis, XRD, thermal, spectroscopic studies and biological evaluation of Co (II), Ni (II) Cu (II) metal complexes derived from 2-benzimidazole *J. Mol. Stru.*,2017;1148:231-237.
18. Nakamoto K, Infrared, Raman. spectra of inorganic and coordination compounds [Internet], in: J. M. Chalmers, P. R. Griffiths (Eds.), *Handbook of Vibrational Spectroscopy*, John Wiley & Sons, Ltd, Chichester, UK, 2006.
19. Murtaza S, Abbas A, Iftikhar K, Shamim S, Akhtar MS, Razzaq Z *et al.* Synthesis, biological activities and docking studies of novel 2,4-dihydroxy benzaldehyde based Schiff base, *Med. Chem. Res.*,2016;25:2860-2871.
20. Joksimovic N, Baskic D, Popovic S, Zaric M, Kosanic M, Rankovic B *et al.* Synthesis, characterization, biological activity, DNA and BSA binding study: novel copper (II) complexes with 2-hydroxy-4-aryl-4-oxo-2-butenate, *Dalton Trans.*,2016;45:15067-15077.
21. Manjuraj T, Yuvaraj TCM, Jayanna ND, Shreedhara SH, Sarvajith MS. Spectral, DFT, molecular docking and antibacterial activity studies of Schiff base derived from furan-2-carbaldehyde and their metal (II) complexes, *J. Turk. Chem. Socty. Chem-A*,2020;7 (2):449-462.
22. Klein E, Lukes V, Ilcin M. DFT/B3LYP study of tocopherols and chromans antioxidant action energetics, *Chem. Phys.*,2007;336:51-57.
23. Rahaman F, Mruthyunjayaswamy BHM. Synthesis, spectral characterization, grain size effect, antimicrobial, DNA cleavage and anticancer activities of cobalt (II), nickel (II), copper (II) and zinc (II) complexes of schiff base, *Comp. Met.*,2014;31:88-95.
24. Yuvaraj TCM, Parameshwara Naik P, Venkatesh TV, Krishnamurthy G, Manjuraj T. Synthesis, spectral studies, XRD, thermal analysis and biological screening of metal complexes derived from (N- (3-methoxyphenyl) -2- [(2E) -3-phenylprop-2-enoyl] hydrazinecarboxamide, *J. Turk. Chem. Socty. Chem-A*,2018;5 (3):845-856.
25. Manjuraj T, Krishnamurthy G, Yadav Bodke D, Bhojya Naik HS. Synthesis, XRD, thermal, spectroscopic studies and biological evaluation of Co (II), Ni (II) Cu (II) metal complexes derived from 2-benzimidazole *J. Mol. Stru.*,2018;1171:481-487.
26. Yuvaraj TCM, Parameshwara Naik P, Venkatesh TV, Krishnamurthy G, Manjuraj T. Synthesis, Characterization, XRD Studies, Molecular Docking and Biological Screening of N-phenyl-2- (pyridin-4-ylcarbonyl) Hydrazine Carboxamide and their 3D Metal Ion Complexes, *Der Pharma Chemica*,2017;9 (19):1-8.
27. Akbari JD *et al.* Synthesis of Some New 1, 2, 3, 4-Tetrahydropyrimidine-2-thiones and Their Thiazolo [3, 2-a] pyrimidine Derivatives as Potential Biological Agents. Phosphorus, Sulfur, and Silicon,2008;183:1911-1922.
28. Weinhardt K, Wallach MB, Marx M. Synthesis and antidepressant profiles of phenyl-substituted 2-amino- and 2- [(alkoxycarbonyl) amino]- 1, 4, 5, 6-tetrahydropyrimidines. *Journal of Medicinal Chemistry*,1985;28 (6):694-698.